6

Photonic Crystal Waveguides and Bio-Sensors

Alessandro Massaro
Italian Institute of Technology IIT
Center for Bio-Molecular Nanotecnology, Arnesano, Lecce
Italy

1. Introduction

Photonic crystals (PCs) are actually implemented as biosensors [Ganesh et al., 2007], optical resonators [Karnutsch et al., 2007] and wavelength filters [D'Orazio et al., 2008; Pierantoni et al., 2006]. Other kinds of photonic crystals can be implemented by considering a periodic structure with defect line and/or central cavities. Several architectures of micro-cavities (see examples in Fig. 1 (a), (b)and (c)) have been studied in the past by using triangular and square lattices layouts [Joannopoulos, 1995] oriented on optoelectronic technology. Optoelectronic technologies are often affected by cost and space problems that prevent them from being used even more widely. The development and implementation of photonic integrated circuits (PICs) could provide a solution to these two major obstacles. Couplers such as tapered waveguides and photonic crystal (PhC) devices can be integrated in the same chip in order to reduce the space, especially concerning complex optical switch systems, and, to provide high transmitted power and high efficiency of the PICs. For example, the use of tapered waveguides is necessary in order couple the light into a W1 PhC waveguide (illustrated in Fig. 1 (a)). This kind of W1 PhC waveguide is object of much interest because of its potential for controlling and manipulating the propagation of light. In particular, sharp bends, junctions, couplers, cavities, add-drop filters, and multiplexers have been experimentally demonstrated or theoretically predicted, thus making these devices very attractive for highly integrated photonic circuits [Mekis et al., 2008; Pottier et al., 2003; Johnson et al., 2002; Sanchis et al., 2002; Chau et al., 2004; Chietera et al., 2004; Xing et al., 2005; Camargo et al., 2004; Talneau et al., 2004; Marki et al., 2005; Camargo et al., 2004; Sanchis et al.,2004; Khoo et al.,2006]. The in-plane coupling of W1 PhC is also an important issue for bio-sensors implemented by micro- and nanofabrication technologies. In fact, the development of micro- and nanofabrication technologies, biomolecular patterning and micro-electromechanical systems (MEMS), has greatly contributed to the realization of miniaturized laboratories applied to genomic and proteomic analysis. The application fields of these biochips are extremely broad, and they have been referred as several different terms (gene-chip, gene-array, DNA microarray, protein chip, and lab-on-chip). Essentially, these chips, developed both in simple stand-alone configurations and integrated devices/architectures, consist of planar structures, realized on several substrates such as glass or plastic materials, where (bio)molecules (such as DNA, proteins or cells, which selectively conjugate with target molecules) can be immobilized on them through chemical surface modification or in situ synthesis [Fan et al., 2006] as happens DNA sensors. These chips require the use of suitable micro-reactors and/or capillary systems, and the

detection of complemental reaction between biomolecular is performed in a solution. Biochip technology has revolutionalized the field of molecular biology, finding broad application regarding the study of gene and protein expressions in several fields such as experimental and clinical diagnostics, biomarker detection, and pharmacogenomics. Actually, several chip setups have been used, such as enzyme assays [Hadd et al., 1997], immunochemistry assays [Wang, et al. 2001], polymorphism detection in genetic variations [Dunn et al., 2000], nucleic acids sequencing [Scherer et al., 1999], chips for the realization of ligase reaction [Cheng et al., 1996], and DNA amplification on micro-volumetric scale [Kopp et al., 1998; Daniel et al., 1998]. In particular, due to the high specificity of the hybridization reaction among the oligonucleotides sequences (complementary base-pairing between adenine and thymine, and guanine and cytosine), chips based on biomolecular interactions among DNA filaments have been developed more rapidly than chips based on proteins. In the latter case, despite of keen interest among the scientific community, it slowed down due to the complex bio-recognition mechanism of proteinaceous molecular species [Bodovitz, 2005].

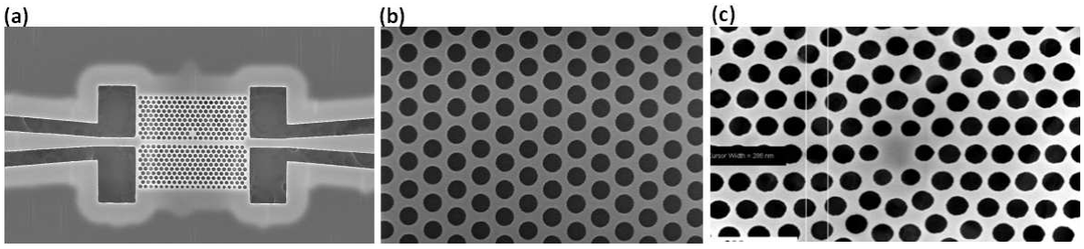

Fig. 1. (a) W1 PhC waveguide. (b) Triangular lattice layout. (c) Circular photonic crystals.

Concerning the discussed topics, we propose to provide examples and design criteria useful to address the reader on the implementation of PhC oriented on bio-applications. The main goal of the chapter is to present an overview about the basic principles of light coupling, light emission and detection approaches of photonic crystals behaving as bio-sensors. In particular, we list below the sections proposed in this chapter.

- The first section analyzes the in plane coupling of tapered waveguides with a PhC waveguide around the working wavelength of 1.31 μm. We first analyze and characterize the coupling between two tapered waveguides, and, then, we model the coupling between tapered waveguides and PhC with micro-cavity. The analysis and the experimental results show the peak frequency shift obtained by varying the taper length. A maximum efficiency of the coupling is reached by a compromise between electromagnetic field confinement and low reflectivity at the input of the coupled photonic crystal. A good agreement with experimental results validates the 2D and 3D numerical results. The proposed in-plane coupling system can be used for W1 bio PhC.
- The second section provides technical advantages of a photonic crystal optical read-out in bio-molecular detection systems (deoxyribonucleic acid (DNA) chips, protein chips, micro-array, and lab-on-chip systems) for genomics/proteomics applications. The proposed method is based on arrays of PhC resonators which contribute to improve a detection efficiency of bio-samples marked with luminescent substances. The detection efficiency is characterized in terms of sensitivity of the analysis, the signal/noise ratio, and speed of the optical read-out process.
- The third section introduces an accurate modeling regarding PhC diffraction efficiency in bio-detection systems. The approach optimizes the detection enhancement of a

luminescent emitting substance located on the photonic crystal which is characterized by a specific emission band. By starting with the analysis of the periodic passive structures it is possible to define design maps in which are reported the diffraction efficiency versus the incidence angles. The PhC is designed to provide a high diffraction efficiency in the emission band of the luminescent substance. In this way the emission of the luminescent substance is enhanced through the high intensity of the zeroth-order backward diffracted wave. These maps could be used to define an admissible error margin due to the uncertainty of fabrication process. The proposed technique can be utilized in different spectral ranges starting from ultra violet to infrared wavelengths, and can be applied to different PhC layouts.

- In the last section we introduce the design criteria for a bio-compatible based polymer PhC suitable as a bio-sensor.

2. In-plane coupling of photonic crystal waveguides

W1 PhC can be obtained by introducing a line defect within the periodic lattice, usually realized through a triangular lattice layout of air holes etched into the substrate. This configuration is compatible with standard planar-semiconductor processing technology. A way to couple efficiently in-plane the light is the use of tapered waveguides. The best geometrical configurations of the tapered profiles are found by performing a good electromagnetic field confinement and low losses. In order to define the frequency response and the electromagnetic coupling of the tapered waveguides, we consider two numerical approach: the finite difference time domain (FDTD) method, and finite element method (FEM). The first one defines accurately the scattered light and the field coupled inside the device, and the second one analyzes the peak frequency resonance and provides the frequency shift versus different taper lengths. This section is organized as follows:

i. we design and model, according with the technological aspects, the optimum tapered waveguide layout (see Fig. 2 (a) and (b)) which couples the electromagnetic field around a working wavelength of λ_0=1.31 μm;
ii. by considering the optimum geometrical configuration of the tapered couplers, we simulate the W1 PhC illustrated in Fig. 2 (c) and (d).

We design integrated tapered waveguides coupled in-plane with an external source (λ_0=1.31 μm) and able to focus the energy in a small waveguide region (ridge of the waveguide).

According with the technological limits (technology resolution) we fix the optical and the geometrical parameters indicated in Fig. 2 (a) and (b) as: D=2μm, d=1.2μm, s=0.3μm, n(GaAs)=3.408, n(AlGaAs)=3.042, w=0.5μm, L_s=16.77 μm. We analyze the bandpass behaviour around the working λ_0=1.31 μm, and evaluate the energy density at the output of the two coupled tapered waveguides. This procedure allows to calculate the best optimum length L of the tapered profile. The inset of Fig. 3 reports a schematic representation of the employed transmission experimental set-up. In this set-up a light probe beam (tungsten broad band lamp) is launched from a tapered fibre and directly injected into the ridge waveguide. The light exiting the waveguide is collected and collimated by a microscope objective with high numerical aperture. The real image of the output facet of the waveguide is then formed on the common focal plane of a telescopic system, where a horizontal slit is placed. This allows us to separate the light coming from the ridge waveguide from the

radiation freely propagating in the air and through the substrate. The transmitted light is collected by a multimode fibre with its free end lying on the focal plane of a lens (end-fire coupling) and brought to an N-cooled InGaAs OMA (optical multichannel analyzer).

As reported in Fig. 4 (2D FDTD simulation) and in Fig. 5 (3D FEM simulation) we have predicted the measured shift of the central wavelength. In our analysis, we have considered four lengths L of the tapered profile (in particular L=25 μm, L=50 μm, L=100 μm, L=200 μm): the central wavelength decreases for the cases L=25 μm to L=50 μm and increases from L=50 μm to L=200 μm. As reported in the 3D FEM results of Fig. 4 and in the 2D FDTD results of Fig. 5, the case of L=50 μm is characterized by a central wavelength far from the working wavelength. Moreover, we observe in the same figures other peaks due to backscattering interference phenomena of the slanted profile. In Fig. 6 we show the comparison between measured, 2D FDTD and 3D FEM spectra by considering L=100 μm: a low error about the central wavelength is observed (the different band amplitudes are due to different kind of light sources). By evaluating the coupled energy at the output of both tapered waveguides, we observe that the cases of L=100 μm and L=200 μm represent the best coupling condition (see Fig. 7 where the energy is defined by the subtended area of the electric field density). in these cases, the losses due to the radiation in the external space are low and, consecutively, the light coupling inside the guiding region is strong (compromise between high transmittivity and low losses at the working frequency). The integral used to evaluate the electric field density of Fig. 7 is:

$$S(t) = \int_V \varepsilon(\mathbf{r}) \left|\mathbf{E}(t)\right|^2 dV \tag{1}$$

Where E is the electric field, ε is the spatial dependent permittivity index, and V is the volume of calculus.

We use for the calculus of (1) as source a carrier modulated by an exponential signal expressed by

$$\Psi_{source} = \exp(-(t \cdot dt / T_0)^2) \cdot \cos(\omega_0 \cdot t \cdot dt) \tag{2}$$

where ω_0 is the angular frequency at λ_0=1.31 μm, T_0 is a constant, and dt is the time step.

We note from numerical results that the 3D FEM results provide better the accuracy of the frequency shift according with the experimental spectra.

We conclude that good choices of tapered waveguides working at λ_0 =1.31 μm are the profiles with L=100 μm and L=200 μm. The field losses can be estimated by introducing a PhC waveguide between the two tapered waveguides as the W1 PhC illustrated in Fig. 8 (a), where the input is coupled through the tapered waveguide with the defect region, and, the signal is coupled with a cavity (as shown by the simulations of Fig. 8 (b) and Fig. 9 (a) illustrating different perspectives of the E_y field component). We analyze as filter a triangular lattice structure characterized by a lattice constant of 0.95 μm and air hole radius of 0.399 μm. In order to confine better the electromagnetic field inside the cavity, the radius of the holes near the cavity are reduced to 0.304 μm (optimization process). In Fig. 9 (b) are illustrated the radiation losses of the whole device using L=100 μm. Moreover the comparison between Fig. 9 (c) and Fig. 9 (d) shows the losses distribution for tapered

waveguides with L=200 μm and helps to discriminate the part of energy irradiated by the photonic crystal from the part irradiated by the tapered profile.

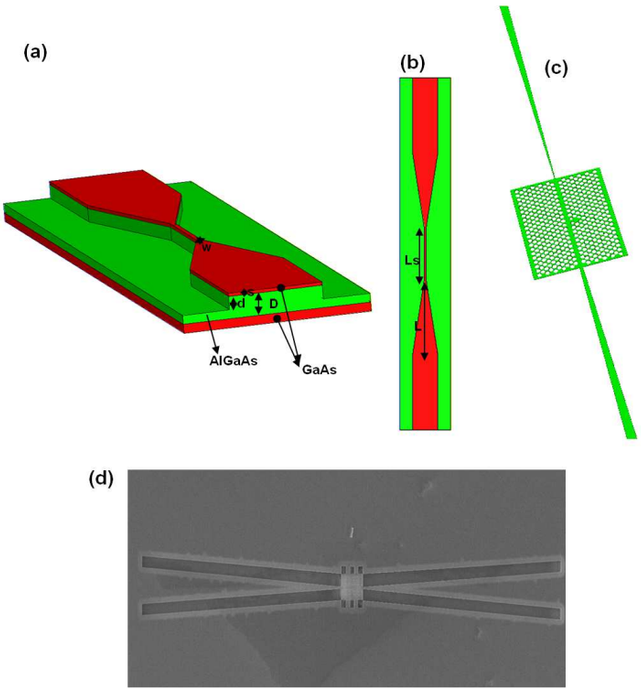

Fig. 2. a) 3D Coupled tapered waveguides; b) top view of coupled tapered waveguide; c) W1 PhC and tapered waveguides. (d) SEM image of the W1 PhC coupled to the input and output by tapered waveguides.

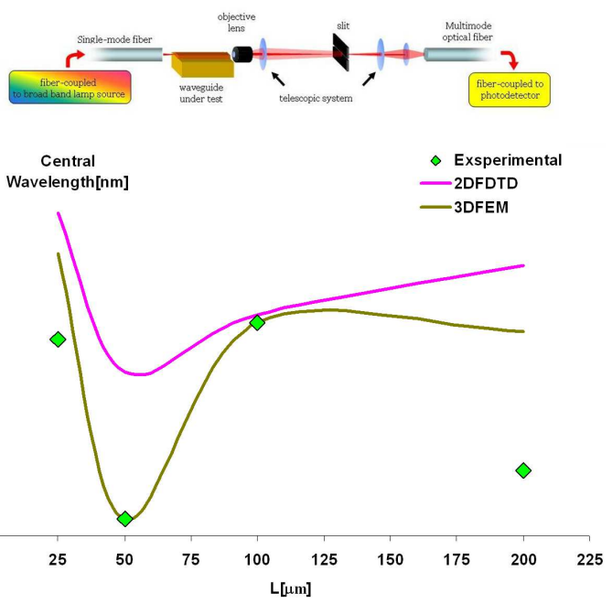

Fig. 3. Central wavelength: comparison between experimental, 2D FDTD and 3D FEM method. Inset: Experimental setup which measures the optical transmittivity of the coupled tapered waveguides of Fig. 1 (a).

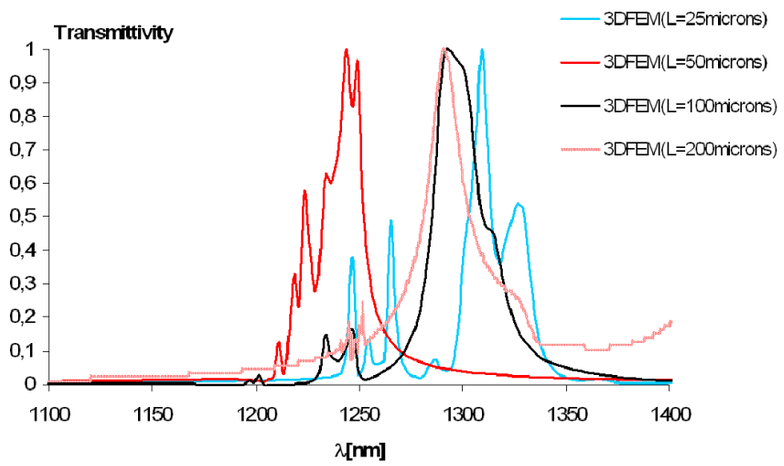

Fig. 4. Wavelength shift: 3D-FEM transmittivity for different lengths L.

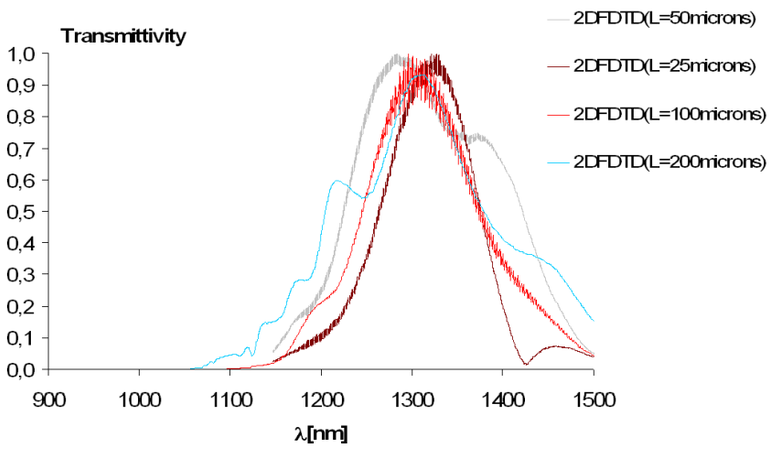

Fig. 5. 2D FDTD spectra comparison.

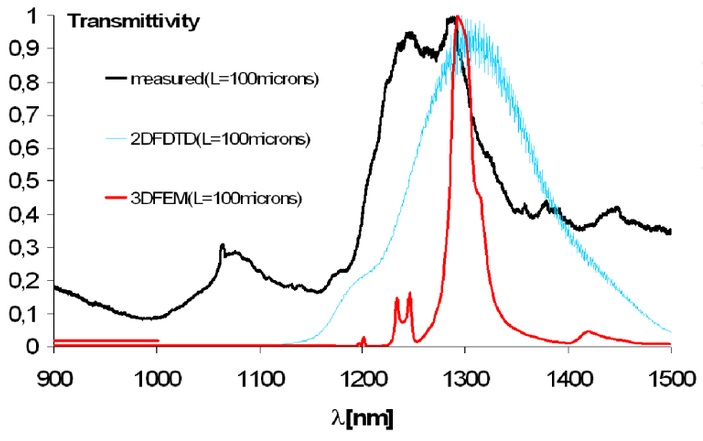

Fig. 6. Comparison between measured, 2D FDTD and 3D FEM spectra of tapered waveguides with L=100 μm.

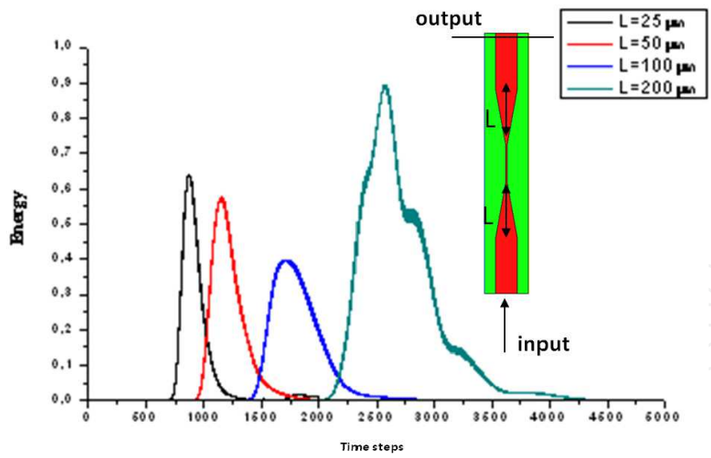

Fig. 7. Density of energy for different taper lengths L at λ_0=1.31µm.

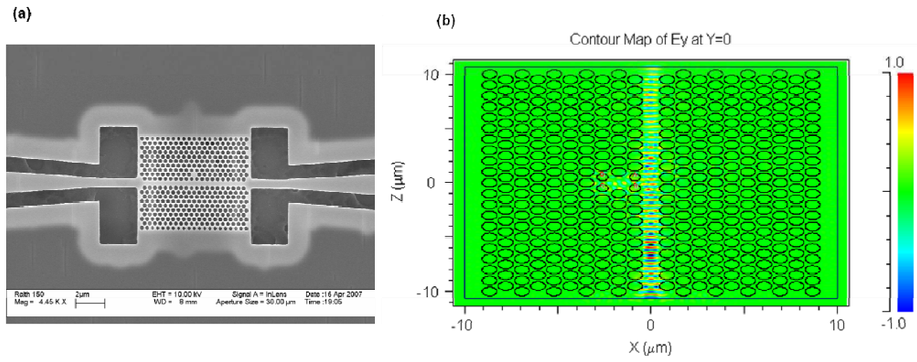

Fig. 8. (a) SEM image of the simulated add drop filter. (b) 2D FDTD simulation of the photonic crystal by using a continuous wave at λ_0=1.31 µm as source.

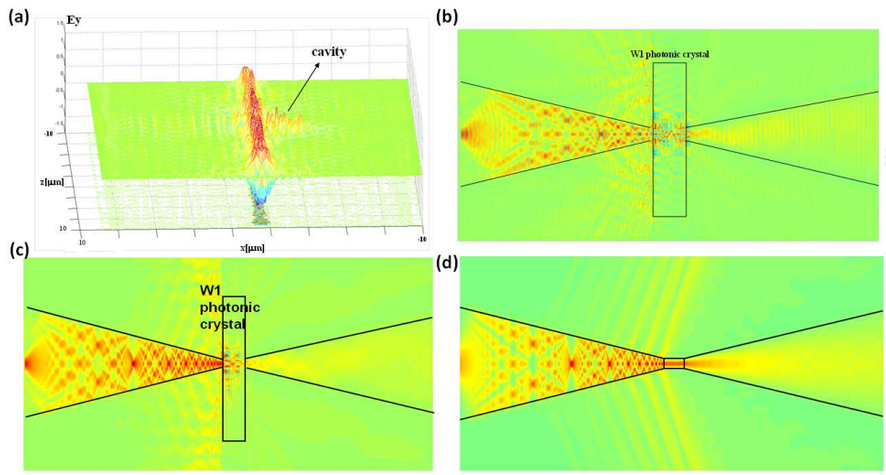

Fig. 9. (a) FDTD simulation: *Ey* component along the W1 region and into the cavity defect. (b) Top view of E_y distribution for tapered waveguides with L=100 µm. (c) Top view of E_y distribution for tapered waveguides with L=200 µm. (d) Top view of E_y distribution for L=200 µm and L_s= 16.77 µm.

3. Photonic crystal resonators array chip for improved optical sensing of (bio) molecules in genomics and proteomics

One of the main goals of this chapter is to analyze the detection efficiency of an optical signal coming from a bio-sensor chip based on luminescence emission. Our approach is based on the employ of arrays of photonic crystals which resonate with emitted lights from a luminous marker associated to a bio-molecule target at a predetermined wavelength. A proper design of these photonic crystal arrays and a spectral analysis of resonant peak emissions allow us to unambiguously associate each analyte to a peak emission, and pick out a useful signal from source reflection/diffraction noise. The use of properly fabricated PhC patterns in an optical read-out region provides us a freedom to modify local spectral distribution of allowed optical modes [Scully et al., 1997]. This concept has been used to increase both excitation and emission efficiencies of optical markers attached on a PhC pattern in bio-molecule detection devices [Mathias et al., 2007]. In particular, in this section we propose to use PhC resonators for a selective enhancement of a luminescent marker-emission only at a specific resonant wavelength. By fabricating several photonic crystal resonators in one bio-chip, each one characterized by a different resonant wavelength and a specific bio-recognition sample attached on each resonator, it is possible to spectrally detect bio-molecule targets in certain positions on a chip. Through the analysis of the total emission spectra collected from the whole read-out area it is thus possible to detect the presence of a certain analyte in a bio-specimen. In comparison with traditional detection systems, based on the spatial scanning of an optical read-out area, this approach permits us to:

a. decrease analysis time. Since the detection of analytes is based on detection of resonant peak emissions, simultaneous measurement on the whole read-out area is possible. This feature allows us to detect analytes through a spectral scanning alone. As the bandwidth of a resonant peak becomes narrower, more peaks can be arranged in a spectrum of a luminous marker. Then, it becomes possible to analyze a larger number of analytes in one time;
b. drastically decrease the reading error caused by diffused, reflected and/or diffracted light source signal;
c. significantly increase the detection sensitivity through the enhancement of the luminescent marker-signal. This enhancement is generated by the coupling of the luminescent light with a resonant mode of PhC patterns. In the proposed system, the unambiguous assignment of a resonant emission to each analyte does not require spatial scanning and/or the use of different fluorescence markers emitting light at different wavelengths. The unambiguous detection is guaranteed by combining each target (bio) molecule with a properly designed PhC resonator. In this way each PhC resonator can manipulate the light emission of a common luminescent marker. This approach can be further extended by utilizing, in the same chip, more than one fluorescent substances simultaneously, with different resonant emission frequencies. Moreover, the proposed technique can be utilized in different spectral ranges, starting from ultra violet to infrared (by utilizing, for example, organic fluorescent substances and/or colloidal nanocrystals) according to the scalability of target wavelengths and scale order of corresponding photonic crystal design [Yablonovitch, 1987; Joannopoulos et al., 1995]. The optical properties of the structure can be modified with a good accuracy in each desired frequency range, by simply changing the geometrical layout of the PhC.

Our optical signal detecting device featuring high sensitivity and multiplexing detection is composed of an array of PhC resonators with specific probes (e.g. single-stranded DNA (ssDNA) sequences, antibodies, receptors, aptamers, etc…) for analytes (e.g. DNA, proteins, ligands, etc.) attached on them. Analytes are trapped with high spatial precision through chemical, physical, electrostatic techniques, and so on (Fig. 10). The target analytes can be directly (e.g. through syntesis) or indirectly marked by conjugation with one or more fluorophores. The basic schemes for a detection of biomolecules (proteins, ligands, etc.) and nucleic acids are shown in Figs. 11 (a) and (b), respectively. To eliminate background noise caused by scattering of excitation light, excitation light can be selectively provided to read-out regions via PhC waveguides. The proposed system is based on a unique optical detection scheme. The detection is performed through the collection of the emission spectrum coming from the whole bio-recognition area of the chip. As previously discussed, by applying a suitable matrix composed by PhC resonators possessing different resonant wavelengths, each bio-recognition element of the device is unambiguously associated to a different resonance peak. By detecting resonant peak emissions at certain wavelengths, it is therefore possible to detect the presence of specific target (bio) molecules contained in the analyzed sample. Thus, it is possible to collect signals from several resonators in a single analysis, increasing the signal collection speed. Moreover, the PhC strongly inhibits the excitation radiation that is diffused or reflected towards the detection direction. Elimination of radiation of excitation light together with the increase in the intensity of the emission signal increases significantly the overall signal-to-noise ratio. This feature helps to reduce reading errors, allowing operators skip the step of complex post-processing to correct read-out errors. Photonic crystals can control the light propagation by introducing a 1D, 2D or 3D periodicity in materials having high optical transparency in the frequency range of interest. Light can be trapped, for instance, by introducing a defect in the periodicity. Summarizing, photonic crystals technology could, therefore, be applied to biochip technology in order to provide the following advantages:

a. controllability of the resonant wavelength of each resonator in the matrix through the accurate material and geometry design. Specifically, it becomes possible to enhance the emission spectrum of the fluorophore conjugated to an analyte. This allows us to perform an optical detection not only on the basis of a spatial discrimination of the different contributions but also on the basis of a spectral discrimination, since each pixel contains a specific optical resonator working at a different frequency.
b. increase of the fluorophore emission efficiency in specific spectral bands through the Purcell effect (e.g. micro resonators with high quality factor (Q-factor) and small modal volume), thus increasing the signal-to-noise ratio.
c. possibility to selectively excite light-emitting marker via waveguides or a resonance of a certain optical mode of photonic crystal to suppress diffused, reflected or diffracted excitation light from the substrate. This can be achieved by controlling the angle of emission or excitation by properly engineering a photonic crystal. This property can be exploited to spatially separate the excitation radiation and the emission band.
d. Regarding point (a), an external excitation light sent towards the matrix at a proper angle will excite the marker bound to the captured analyte, which will emit its typical broad signal. Then, the broad emission is peculiarly amplified in specific spectral bands by the underlying pixel with a photonic crystal resonator (Fig. 12 (a)). The variation from pixel to pixel (that is, from analyte to analyte), of the frequencies contemporarily

emitted from the matrix allows a high degree of parallelism on a high number of different analytes, thus also fastening the recognition of the examined samples.

Regarding points (b) and (c), the proper choice of both the materials and the photonic crystal geometry can lead to the realization of a photon energy bandgap. As already mentioned, it is possible to localize specific optical modes to confine them in a small defect region in the photonic crystal. Only the modes which resonate in this small region will be amplified. Photonic crystal cavities are, therefore, designed to separate the useful signal coming from the biological assay from the noise coming from excessive source light. Then, we can obtain very sharp optical signals which are easily recognized thanks to their amplified intensity together with the spectral scanning of the detection system. Figs. 12 (b) and (c) show examples of an intact emission spectrum from a read-out region and signals collected from several read-out regions assisted by the array of photonic crystal resonators, respectively. The presence of each peak in the ensemble spectrum of Fig. 12 (c) reveals the presence of the corresponding target analyte in the analyzed assay. A further spatial separation between the scattered excitation light and a signal can be achieved by providing the excitation light to a read-out region or extracting the excited light from a read- out area through suitable waveguides. In this sense, the PhC can be designed to selectively guide light between resonators and detectors [Aoki et al., 2009].

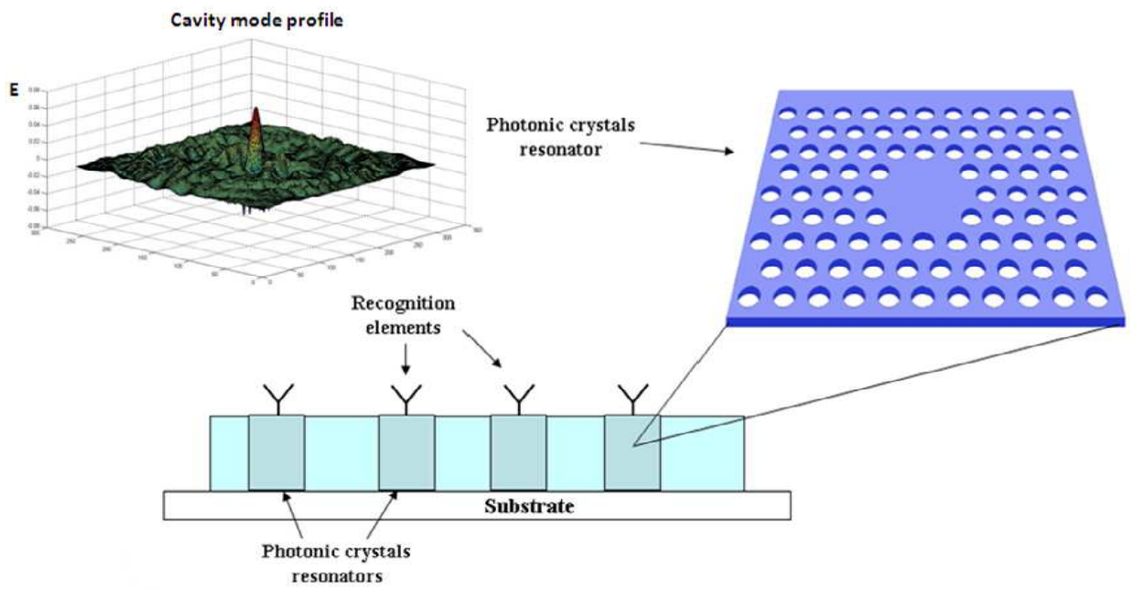

Fig. 10. Schematic of the optical transducer for biomolecular analysis in genomics/proteomics. The proposed device is essentially characterized by a substrate on which are realized arrays of resonant photonic crystals. On the surface of each resonator specific bio-molecules are fixed (for example, through chemical functionalization), which behave as target probes for the analytes to be detected. In the sketch there have been shown, as an example, arrays of photonic crystal and bio-molecules of the same typology. It is obviously possible to consider, in the same chip array, different photonic crystal structures with different wavelength resonances. Analogously, each bio-recognition element bound on the single resonator can be different from each other, and peculiar for each analyte.

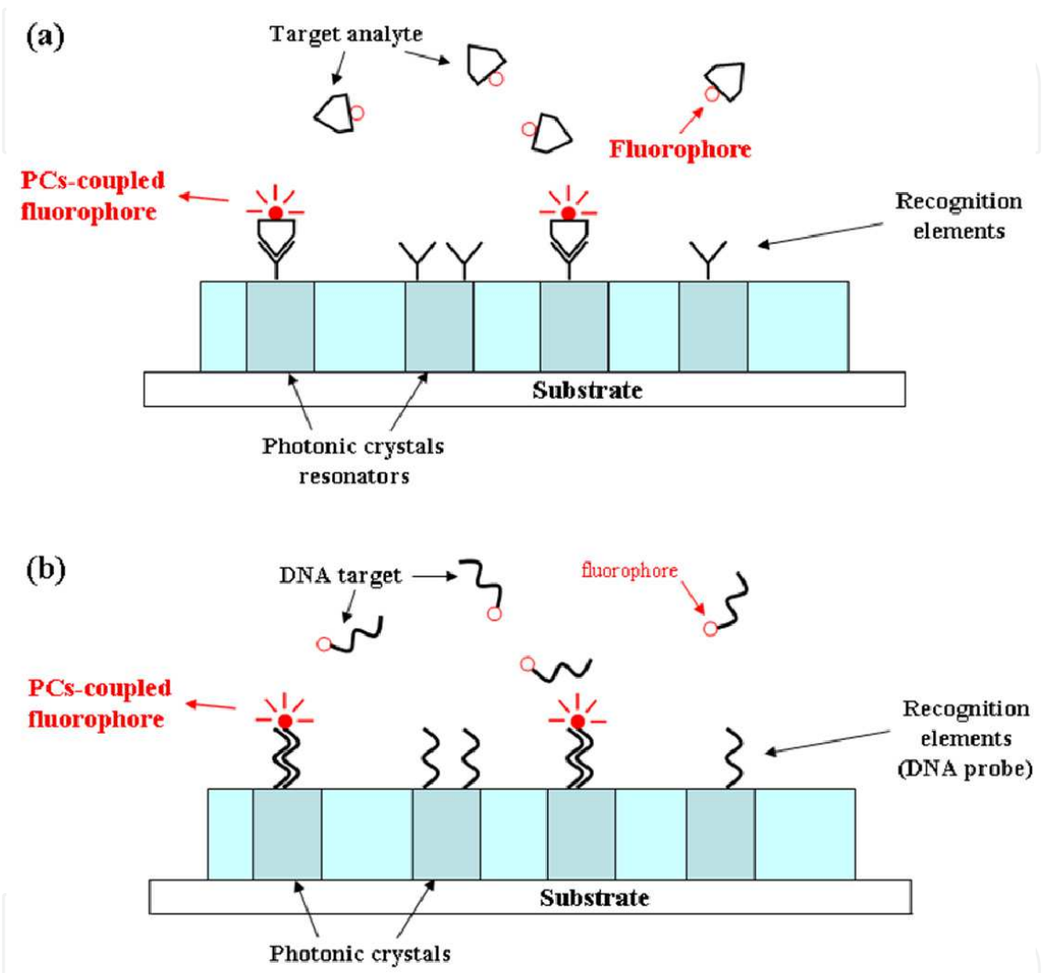

Fig. 11. Schematics of the optical transducer for the analysis of biomolecules in genomics/proteomics. (a) General sketch including a selective bio-recognition element for a specific target analyte (oligonucleotides, proteins, ligands, etc.). (b) Example of a devices suitable for DNA analysis: in this case, the probe bound to the resonator surface is a specific ssDNA sequence. Similarly to the above description, the resonators can differ from each other, as far as the (bio) recognition elements (for instance, the DNA probe) bound to each resonator, in order to perform spectral multiplexing analysis.

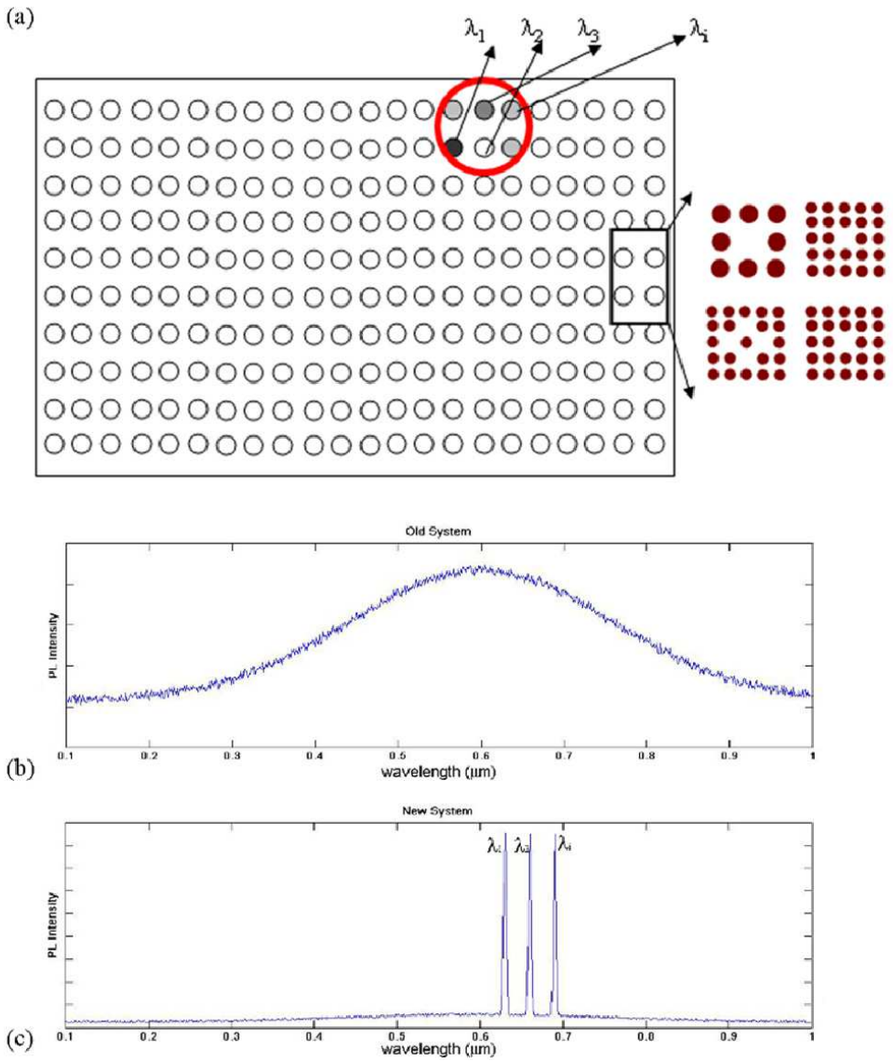

Fig. 12. (a) Schematics of a photonic crystal resonators matrix used in the optical DNA micro array chip. Each resonator of the matrix (bounded to a specific bio-recognition element) is designed in order to show a different resonant wavelength. (b) A typical example of the emission collected from a read-out area not assisted by photonic crystal resonators. The line-shape is typical of the original marker, with the presence of a significant noise due to scattered excitation light. (c) Example of the emission signal detected on the whole read-out area, where λ_1, λ_2 and λ_i are the spectral peculiar modifications due to the coupling of the fluorophores with the 1st, 2nd and ith resonator in the matrix. The presence of each peak in the ensemble spectrum reveals the presence of the corresponding target analyte in the analyzed assay.

4. Diffraction efficiency modeling of 2D photonic crystals for biosensing applications

Optical bio-sensing approach usually consists of light intensity detection systems. Typically, the luminescent signal is emitted by a luminescent marker conjugated to the bio-target. A

good enhancement of this emitted signal can be obtained by combining a PhC structure with the luminescent substance. The signal enhancement can be optimized by analyzing the diffraction efficiency of the light emitted from the luminescent substance, characterized by the **K** wave-vector (see Fig. 13 (a) and (b)). In general, by exciting a properly designed PhC structure with an optimum incidence angle, it is possible to detect a high-intensity diffracted signal. The presented diffraction modeling takes into account this optimum incidence condition by defining sets of possible incidence angles (working regions) in the emission luminescent band. In this section the diffraction efficiency of a square lattice PhC Si_3N_4 membrane covered with a luminescent substance is modelled. The structure is excited by a plane wave and the light coming out from the luminescent substance is also modeled as a plane wave with the **K** vector shown in Fig. 13 (a), characterized by θ and ϕ angles. In Fig. 14 (a) and (b) we report the diffraction efficiency map versus the wavelength and the ϕ angle for different launch θ-angles. By fixing the θ and ϕ angles in the working region (see Fig. 14 where ϕ=θ=30°), it is possible to analyze the sensitivity of the reflectivity response. This allows to estimate the error margins due to the limits of the fabrication technology and of the experimental setups. As example, in Fig. 15 (a) is reported the sensitivity of the reflectivity response by varying hole radius in steps of 5 nm. Transverse electric (TE) and transverse magnetic (TM) PhC radiation modes define the diffraction concerning different PhC Brillouin directions. Figure 15 (b) shows the TM PhC radiation modes (diffraction modes) in the luminescent emission band 0.56μm≤λ≤0.58μm. The PhC Si_3N_4 membrane structure is excited by a plane wave and the light coming out from the luminescent substance, is collected in a detection system.

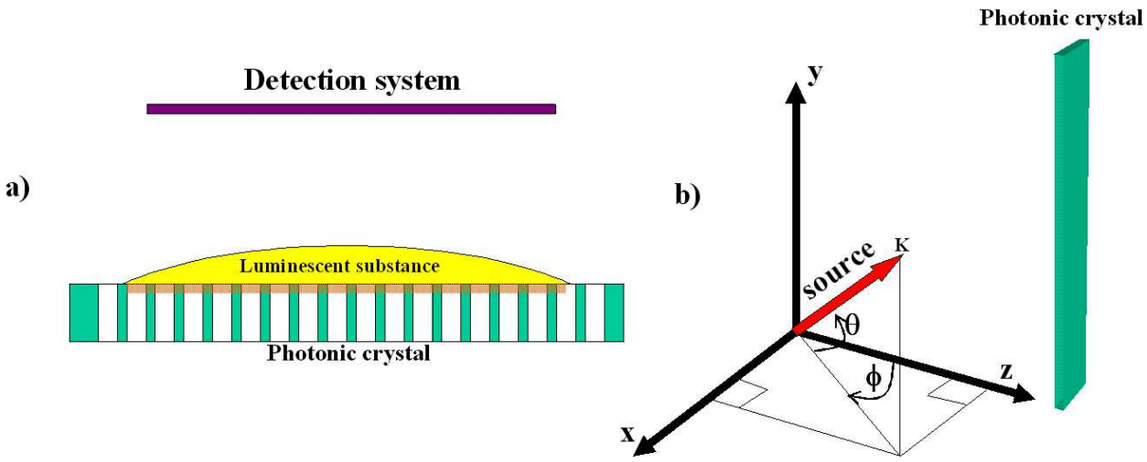

Fig. 13. (a) Photonic crystal for bio-sensing applications. (b) Source launch coordinate system of the model.

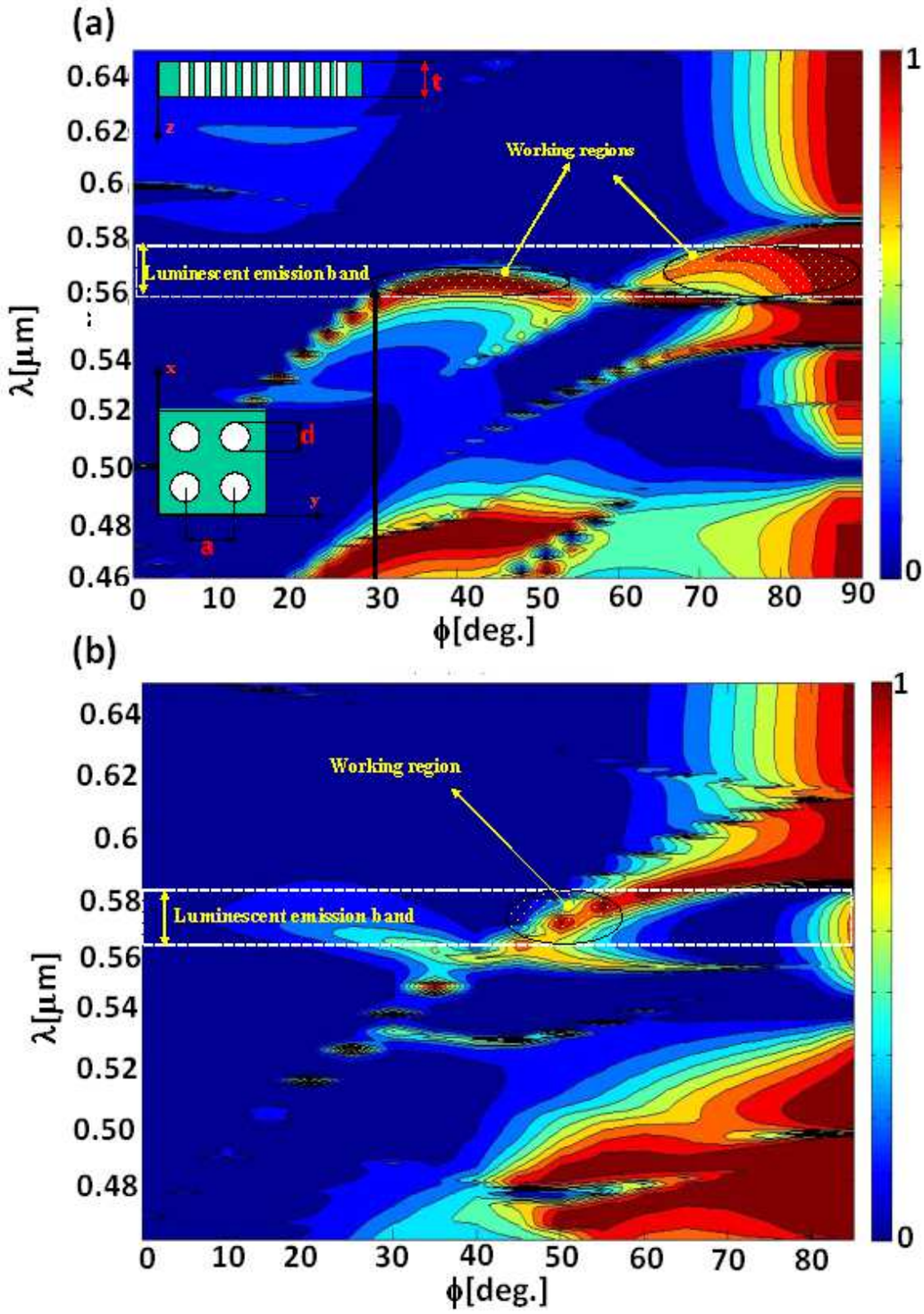

Fig. 14. Diffraction efficiency map versus λ and ϕ angle: d=180nm, a=300nm, t=300nm, θ=30 deg. Diffraction efficiency map versus λ and ϕ angle: d=180nm, a=300nm, t=300nm, θ=45 deg.

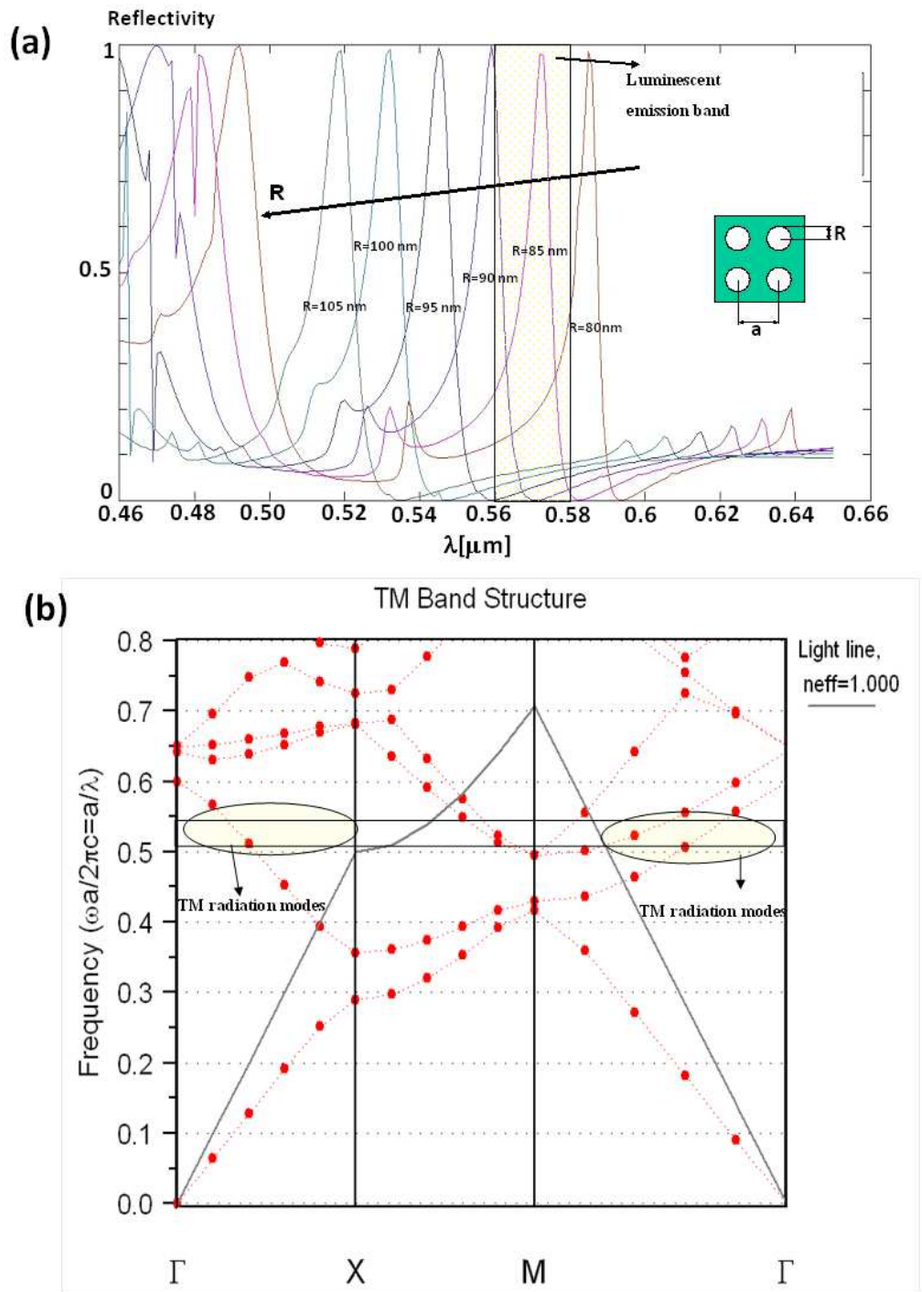

Fig. 15. Reflectivity of a 2D periodic structure versus the air hole radius R (*a*=300nm, *t*=300nm). Example of TM radiation modes for a square lattice PhC with *a*=300nm.

5. Design criteria of a biocompatible polymeric photonic crystal sensor and discussions

Concerning bio compatible PhC, we consider in the example of this section, gold pillars growth on Polydimethylsiloxane (PDMS) polymer. In order to improve resonant emitting peaks, we fix as example a square lattice layout with a central micro-cavity defect (see Fig.

16 (a)) [Massaro, 2011]. The input is a laser beam working at a wavelength λ. The source excites in the PhC waveguides TE and TM modes characterized by the electromagnetic field components reported in Fig. 16 (b). The PDMS material ($n_{background}$=1.4) represents the background where will be growth the gold pillars. The design criteria in order to improve efficient emitting cavities are listed by the following points:

1. we define the band gaps of the PhC without micro-cavity defect;
2. we calculate the band gaps of the same PhC with central defect obtained by omitting the central pillar;
3. we define the mode distribution of the cavity modes.

By focusing on TE modes we calculate the band gaps illustrated in Fig. 17 (a). Then we introduce the central defect as indicated in Fig. 16 (a) and calculate the new band gaps by observing that one of previous band will be divided into two band gaps. In the analyzed case, the band gap found around a/λ = 0.3 is divided into two ones as shown in Fig. 17 (b). The cavity modes are defined between the two new band gaps. The cavity modes are confined inside the cavity as proved by Fig. 18 which illustrates the modal profiles of the electric field component E_y . It is possible to select the best cavity modes (characterized by the best quality factor) by tuning the source wavelength around the selected mode. In order to improve strong power energy inside the cavity, we excite the PhC slab by a TE polarized source. The light emitting property along the direction orthogonal to the layout plane, could be improved by considering a 3D membrane type configuration or a central defect pillar characterized by a different size or material. The 2D approach allows to mainly fix the geometrical layout and to define the working wavelength. An accurate study of the 3D model will supply information about the best geometrical parameters such as the height of the pillars, the PDMS slab core thickness, and the dimensions of the membrane [Massaro et al., 2008]. Possible measurements of the designed PhC can be performed by Micro-photoluminescence setup [Massaro et al., 2008], by Fourier transform infrared (FTIR) and by UV visible analysis.

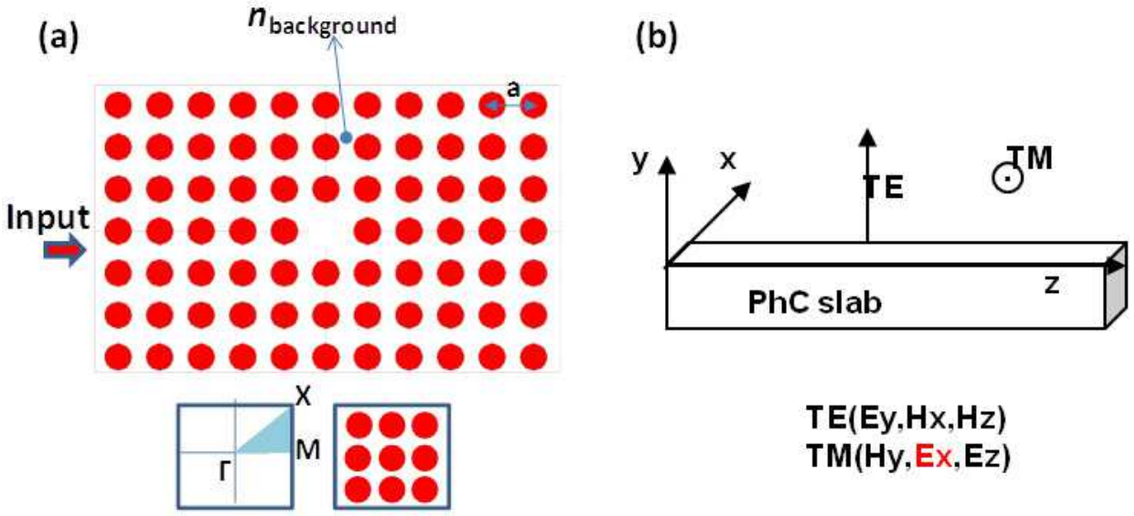

Fig. 16. (a) Example of square lattice 2D layout of a PhC with central micro-cavity and gold pillars. (b) TE and TM mode classification.

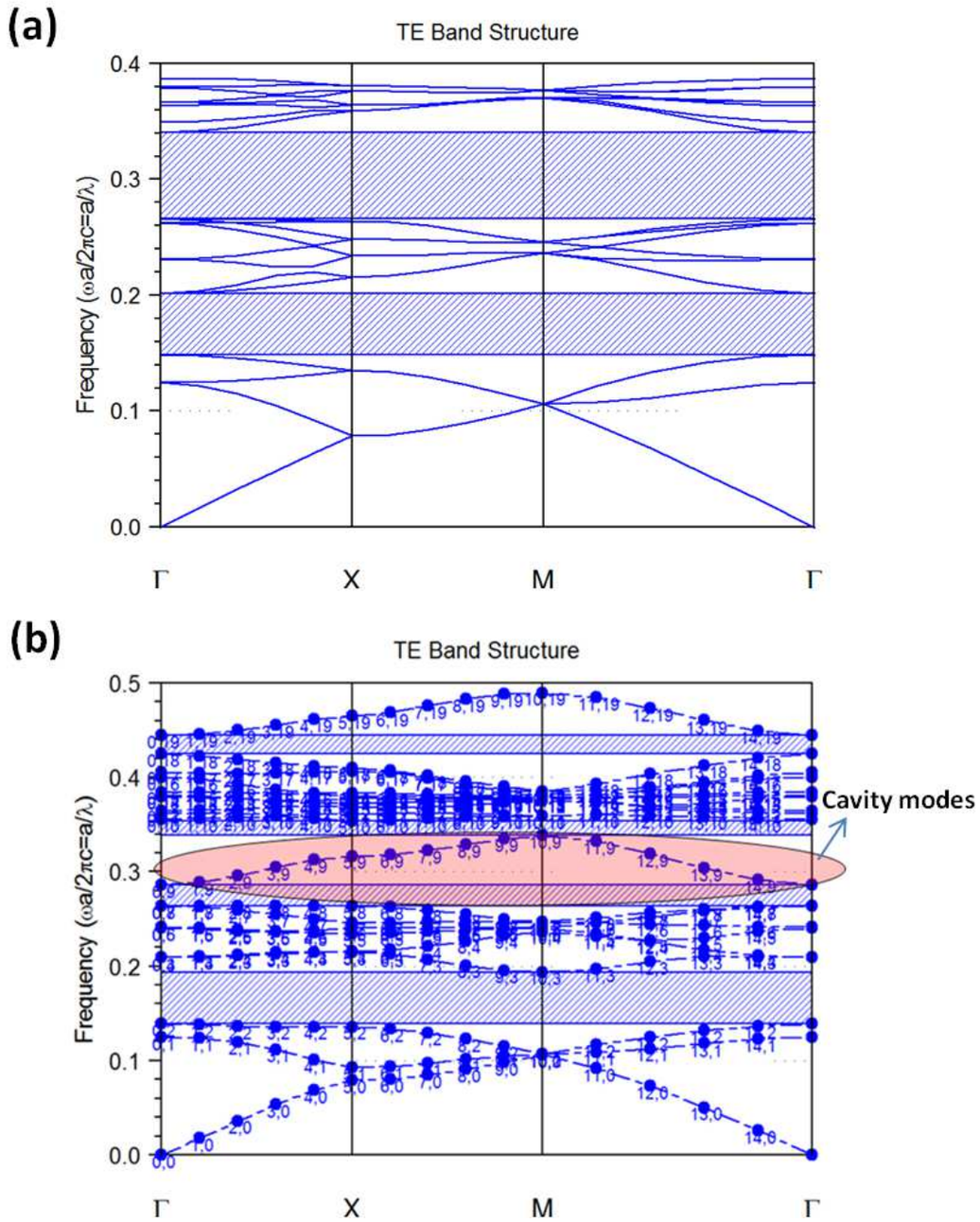

Fig. 17. (a) TE Band diagram of square lattice PhC without (a) and with (b) micro-cavity central defect, respectively.

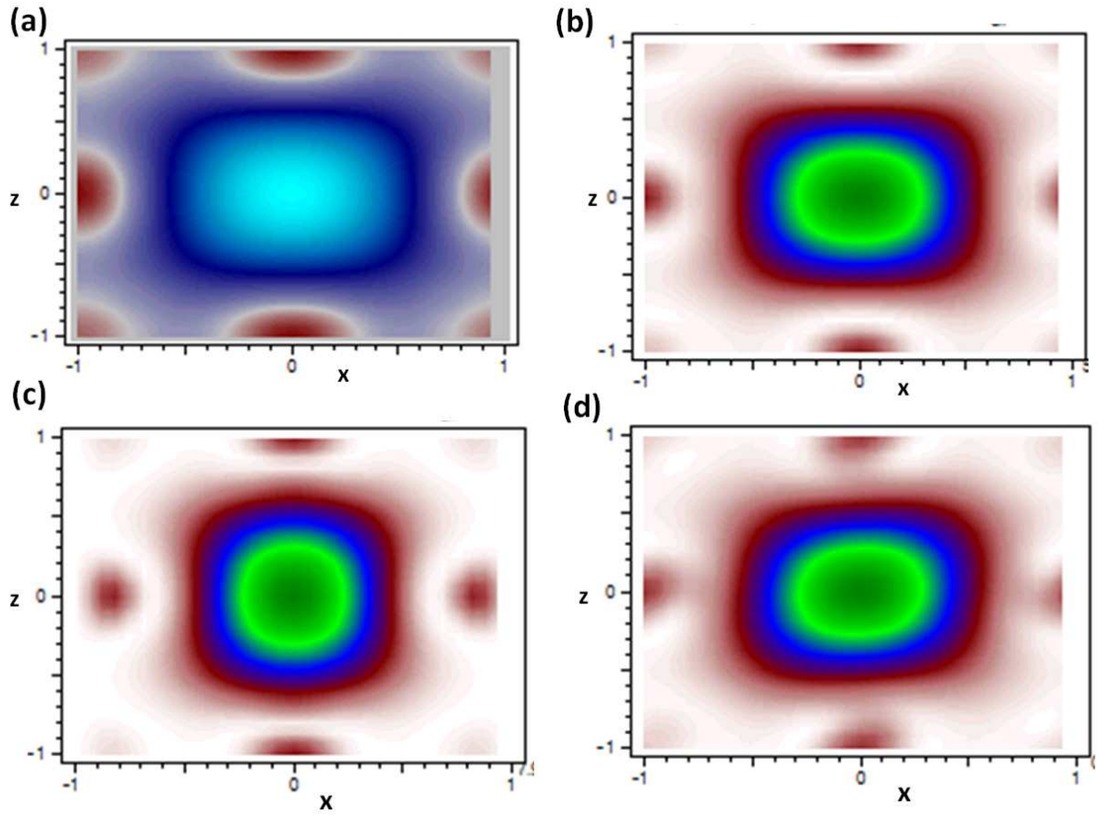

Fig. 18. Cavity mode profiles of modes indicated in Fig. 17: (a) mode 0.9; (b) mode 2.9; (c) mode 11.9; (d) mode 14. 9.

6. Conclusion

Examples of photonic crystal waveguides and bio-sensors are presented. The main goal of the proposed chapter is to provide information about methods and approaches of bio-sensing systems. In the first part of the chapter we focus on the in-plane coupling of a light source by analyzing different tapered waveguide profiles able to couple W1 photonic crystals. Then we analyze different bio-sensors such as DNA sensor chip and PhC Si_3N_4 membrane, by discussing the irradiation and diffraction properties. In the last part we provide design criteria of a bio-compatible polymeric PhC.

7. Acknowledgment

The author would like to appreciate the NNL, Istituto di Nanoscienze - CNR for the support received during my past research activity.

8. References

Aoki K., Vittorio M., Stomeo T., Pisanello F.,Massaro A., Martiradonna L., Sabella S., Rinaldi R., Arakawa Y., Cingolani R., Pompa, P., (2009), EP 09166989.5-1234.

Bodovitz, S., Joos, T., & Bachmann, *J. DDT*, Vol. 10, (2005), No. 4, pp. 283.

Camargo E. A. Chong, H. M. H. & De La Rue, R. Four-port coupled channel-guide device based on 2D photonic crystal structure. *Photon. Nanostruct.*, (2004), pp. 207.

Camargo, E. A.; Chong, H. M. H. & De La Rue, R. M. 2D Photonic crystal thermo-optic switch based on AlGaAs/GaAs epitaxial structure. *OSA Opt. Express*, Vol. 12, (2004),No. 4, pp. 588.

Chau, Y.-F.; Yang, T.-J.; & Gu, B.-Y. Significantly enhanced coupling Efficiency in 2D Photonic crystal waveguides by using cabin-side-like tapered structures at two terminals. *J. Appl. Phys.*, Vol. 43, (2004), pp. 1064.

Cheng, J., Shoffner, M.A., Mitchelson, K.R., Kricka, L.J., & Wilding, P., *J. Chrom. A* , Vol. 732, (1996), No. 1, pp. 151.

Chietera, G.; Bouk, A. H.; Poletti, F; Poli, F.; Selleri, S. & Cucinotta, A. Numerical design for efficiently coupling conventional and photonic-crystal waveguide. Microwave Opt. Technol. Lett., Vol. 42, (2004), No. 3, pp. 196.

D'Orazio, A.; De Sario, M.; Marrocco, V.; Petruzzelli, V. & F. Prudenzano. Photonic crystal drop filter exploiting resonant cavity configuration. *IEEE Trans. Nanotechnol.*, Vol. 7, (2008), pp. 10.

Daniel, J.H et al., Sensors and Actuators A: Physical ,Vol. 71,(1998) ,No. 1-2, pp. 81-88.

Dunn, W.C. et al., *Anal. Biochem*. Vol. 277, (2000), No. 1, pp. 157.

Fan, J.-B., Chee, M.S., & Gunderson K.L., *Nature Review Genetics* Vol. 7, (2006), pp. 632.

Ganesh, N.; Zhang, W.; Mathias, P. C.; Chow, E.; Soares, J. A. N. T.; Malyarchuk, V.; Smith, A. D. & Cunningham B. T. Enhanced fluorescence emission from quantum dots on a photonic crystal surface. *Nature Nanotechnol.*, Vol. 2, (2007), pp. 515.

Hadd, A.G. et al., *Anal. Chem*. Vol. 69, (1997) ,No.17, pp. 3407.

Joannopoulos, J. D., Meade, R. D., and Winn J. N. Photonic Crystal –Modeling the Flow of Light. Princeton University Press, (1995).

Johnson, S. G. ; Bienstman, P.; Skorobogatiy, M. A.; Ibanescu, M.; Lidorikis, E.; & J. D. Joannopoulos. Adiabatic theorem and continuous coupled-mode theory for efficient taper transitions in photonic crystals. *Phys. Rev. E*, Vol. 66, (2002), pp. 1.

Karnutsch, C.; Stroisch, M.; Punke, M.; Lemmer, U.; Wang, J. & Weimann, T. Laser diode-pumped organic semiconductor lasers utilizing two-dimensional photonic crystal resonators," *IEEE Photon. Technol. Lett.*, Vol. 19, (2007), pp. 741.

Khoo, E. H. ; Liu, A. Q. & Wu J. H. Modified step-theory for investigating mode coupling mechanism in photonic crystal waveguide taper. *OSA Opt. Express*, Vol. 14,(2006), No. 13, pp. 6035.

Kopp, M.U., de Mello, A.J., & Manz, A., *Science* , Vol. 280, (1998), No. 5366, pp. 1046.

Marki, I.; Salt, M.; Herzig, H. P.; Stanley, R.; El Melhaoui, L.; Lyan, P. & Fedeli, J. M. Characterization of buried photonic crystal waveguide and microcavities fabricated by deep ultraviolet lithography. *J. Appl. Phys.*, Vol. 98, (2005), pp. 1.

Massaro A., "Theory, Modeling, Technology and applications of Micro/Nano quantum electronic and photonic devices," Transworld Research Network, IBN: 978-81-7895-498-1, 2011.

Massaro, A., Errico, V., Stomeo, T., Salhi, A., Cingolani, R., Passaseo, A. & De Vittorio M. 3D FEM Modeling and Fabrication of Circular Photonic Crystal Microcavity. *IEEE J. Light. Technol.*, Vol.26, (2008), No. 16, pp. 2960.

Mathias, P.C., Ganesh, N., Chen, L.L. & Cunningham, B.T., *Appl. Opt*. Vol. 46, (2007), pp. 2351.

Mekis, A. & Joannopoulos, J. D. Tapered couplers for efficient interfacing between dielectric and photonic crystal waveguide. *IEEE J. Light. Technol*., Vol. 19, No.,(2001), pp. 861.

Pierantoni, L.; Massaro, A. & Rozzi, T. Efficient Modeling of a 3D-Photonic Crystal for Integrated Optical Devices. *IEEE Photonics Technology Letters*,Vol.18, No.2, (2006), pp.319.

Pottier, P.; Ntakis, I.; De La Rue, R. M. Photonic crystal continuous taper for low-loss direct coupling into 2D photonic crystal channel waveguides and further device functionality. *Opt. Comm*., Vol. 223,(2003), pp. 339.

Sanchis, P.; Garcia, J.; Marti, J.; Bogaerts, W.; Dumon, P.; Taillaert, D.; Baets, R.; Wiaux, V.; Wouters, J. & Beckx, S.. Experimental demonstration of high coupling efficiency between wide ridge waveguides and single-mode photonic crystal waveguides. *IEEE Photon. Techn. Lett*., Vol. 16,(2004), No. 10, pp. 2272.

Sanchis, P.; Martì, J.; Blasco, J.; Martinez, A.; & Garcia, A. Mode Matching technique for highly efficient coupling between dielectric waveguides and planar photonic crystal circuit. *OSA Opt. Express*, (2002), Vol. 10, No. 24, pp. 1391.

Scherer, J.R.et al. *Electrophoresis* Vol. 20, (1999), No. 7, pp. 1508.

Scully, M.O. & Zubairy, M.S. Quantum Optics. *Cambridge University press*, Cambridge, 1997.

Talneau, A.; Mulot, M.; Anand, S.; Olivier, S.; Agio, M.; Kafesaki, M. & C.M. Soukoulis. Modal behavior of single-line photonic crystal guiding structures on InP substrate. *Photon. Nanostruct*., (2004), pp. 1.

Wang, J., Ibanez, A., Chatrathi, M.P., & Escarpa, *A., Anal. Chem*. Vol. 73, (2001), pp. 5323.

Xing, A.; Devanço, M.; Blumenthal, D. J. & Hu, E. L. Transmission measurements of tapered-single line defect photonic crystal waveguide. *IEEE Photon. Techn. Lett*.,Vol. 17, (2005),no. 10, pp. 2092.

Yablonovitch, E., *Phys. Rev. Lett*. Vol. 58, (1987), pp. 2059.

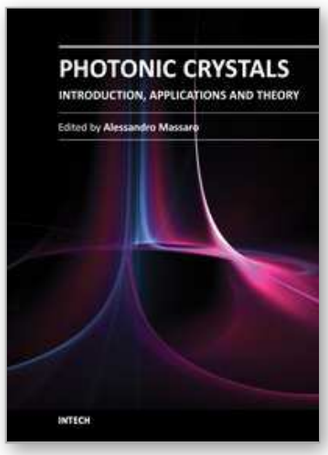

Photonic Crystals - Introduction, Applications and Theory
Edited by Dr. Alessandro Massaro

ISBN 978-953-51-0431-5
Hard cover, 344 pages
Publisher InTech
Published online 30, March, 2012
Published in print edition March, 2012

The first volume of the book concerns the introduction of photonic crystals and applications including design and modeling aspects. Photonic crystals are attractive optical materials for controlling and manipulating the flow of light. In particular, photonic crystals are of great interest for both fundamental and applied research, and the two dimensional ones are beginning to find commercial applications such as optical logic devices, micro electro-mechanical systems (MEMS), sensors. The first commercial products involving two-dimensionally periodic photonic crystals are already available in the form of photonic-crystal fibers, which use a microscale structure to confine light with radically different characteristics compared to conventional optical fiber for applications in nonlinear devices and guiding wavelengths. The goal of the first volume is to provide an overview about the listed issues.

InTech Europe
University Campus STeP Ri
Slavka Krautzeka 83/A
51000 Rijeka, Croatia
Phone: +385 (51) 770 447
Fax: +385 (51) 686 166
www.intechopen.com

InTech China
Unit 405, Office Block, Hotel Equatorial Shanghai
No.65, Yan An Road (West), Shanghai, 200040, China
中国上海市延安西路65号上海国际贵都大饭店办公楼405单元
Phone: +86-21-62489820
Fax: +86-21-62489821

IntechOpen